Journal of Imaging Science and Technology® 52(2): 020505–020505-6, 2008.

Sub-Pixel Retinal Vessel Tracking and Measurement Using Modified Canny Edge Detection Method

Samuel H. Chang▲ and Duk-Sun Shim
School of Electrical and Electronics Engineering, Chung-Ang University, Seoul 156-756, South Korea
E-mail: chang@sisinc.org

Abstract. *This article presents a new method to track and measure retinal blood vessel with sub-pixel accuracy. The method is based on a modified Canny edge detection method and a Gaussian model of the vessel profile and zero cross of second order derivative of the Gaussian model. In this method, Canny edge detection method is used at first to detect edges from an input retinal image. The edge orientation is then refined and used to obtain vessel cross-sectional profile. Vessel sample profile is searched using local maximum and local minimum from the smoothed vessel cross-sectional profile. Gaussian model is then used to fit the vessel sample profile. The zeros cross of the second order derivatives of the Gaussian fit vessel sample profile are then used to represent the boundaries of the blood vessels. The peaks of the Gaussian fits are then used as positions of vessel center lines and to calculate the widths of the vessel at those points. The method outputs vessel wall positions, the center lines of the vessels with the widths of the vessels with respect to center points in sub-pixel accuracy. © 2008 Society for Imaging Science and Technology.*
[DOI: 10.2352/J.ImagingSci.Technol.(2008)52:2(020505)]

INTRODUCTION

Tracking based approaches is one of the important vessel segmentation algorithms.[1] In retinal vessel detection, there are two important issues on vessel tracking and measurements: first, to detect the locations of the vessel boundaries, and second, to track the center lines of the vessels and to measure the width of the vessel at each center point. Both edge detection and matched filter have been used to track the retinal vessels. To detect the right and left edges of the vessels, parallel edge detection makes use of a bar-shaped model of lines. Traditional line detection methods have been used to track parallel edges[2,3] or to find ridges.[4–6] Edge detectors such as Canny detector[7] and Sobel detector[8] are widely used to detect vessel boundaries. Morphological detector,[9] gradient operator,[10] directional matched low-pass differentiator template[11] and optimized Canny's detector[12] were also used to detect vessels. To extract the centerlines of the vessels, the fitness of estimating vessel profiles with Gaussian function has been used.[13] Vessel profile was described by modified Gaussian model that takes into account the central light reflection of arterioles[14] and the vessel measurement was done using amplitude-modified second-order Gaussian filter.

Canny edge detection technique is based on the magnitudes and orientations of local gradients and not directly based on image intensity. It can detect vital anatomical features in retinal images robustly without any enhancement process and compensation of irregularities of illumination by Gaussian smoothing and has been used to extract the boundaries and detect the edges of vessels,[15–20] and to segment different textures and background.[21,22]

There are advantages using Canny edge detector finding vessel positions. First, it minimizes the probability of false positives and false negatives. Second, it detects edges close to the vessel walls and, finally, it returns edge for vessel wall point. However, there are limitations on this application. First, Canny edge detection is local even it filters out the image noise using convolution with derivative of Gaussian and searches connected components with some local connections under certain conditions. The gradient magnitude and orientation estimation is based on local derivatives of x and y directions. The changes of orientation of the gradient from one edge point to another may not be continuing. In most of the cases of blood vessel extractions, the edge positions are far from smooth comparing with the real blood vessels. Second, Canny detector chooses an edge pixel based on local maximum of magnitude gradient satisfying some threshold values and neighborhood information, edges lying on one side of the vessel wall may be missing when either the signal is too weak or the changes of gradients in two sides of a vessel are different. Center lines extracted based on the unsmoothed Canny edges of vessel walls are not smooth and the width measurements are not accurate. Figure 2 shows an edge orientations vector field over a vessel image based on vessel curve extracted from Canny edge detector. The travel directions along the vessel wall are not smooth.

To solve these problems, a filter is used to smooth the edge orientation vector field and the measurements are then done based on the smoothed vector field. In our algorithm, the candidate boundaries of the blood vessel are first extracted using Canny edge detector. Then, the edge locations are used as priori knowledge about the retinal vessel properties to search for one-dimensional (1D) vessel cross-sectional profile, and then, the edge points are tracked into curves, and the smoothed curves are then used to refine the edge orientations. The vessel cross-sectional profiles are then

▲IS&T Member.

Received Nov. 5, 2007; accepted for publication Jan. 17, 2008; published online Apr. 2, 2008.
1062-3701/2008/52(2)/020505/6/$20.00.

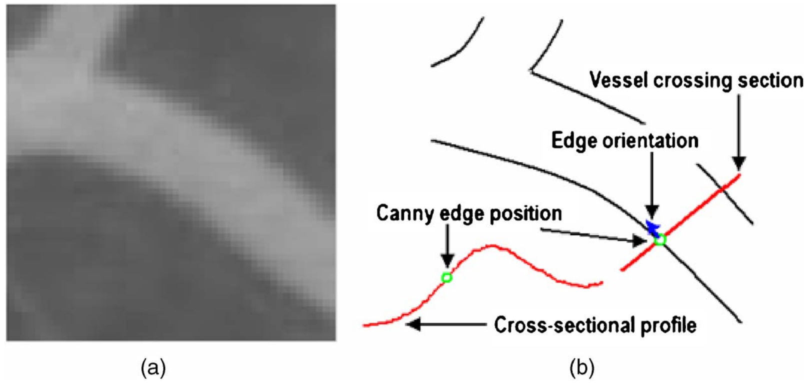

Figure 1. A small region of a retinal image (a) shows a sample of a blood vessel. The pixel locations and orientations of vessel walls can be extracted using Canny edge detector shown in (b).

found through the edge point perpendicular to the edge orientation and then smoothed. Then the vessel sample profile is searched using local maximum and local minimum from the smoothed vessel cross-sectional profile. The vessel profile is modeled by a Gaussian fit function. A sub-pixel accurate edge location is then estimated by using zero cross of the second order derivative of Gaussian fit function. The center point of the vessel is then tracked based on the peak of the Gaussian fit function. The width of the vessel at this point is then calculated based on the distance between the new edge and the center point.

Our algorithm is developed based on the following observed properties of blood vessels in the retinal images:[23] (1) the density distribution of a blood vessel cross-sectional profile can be estimated using a Gaussian shaped function; (2) the vessel segment direction varies continuously, the change of direction between segments is a smooth continuous function; and, (3) the width of the vessel varies continuously and there is no step change in the width of vessel segments. There is always a smooth transition between adjacent segments under the experimental assumption that vessel width is a function of the matched filter when the magnitude coefficient of the filter is suitably assigned. Then the absolute value of vessel diameter can be determined simply by using a pre-calibrated line.

The latest work similar to our algorithm is the approach of Li et al.[24] In their approach, the detected vessels are traced with the help of a combined Kalman filter and Gaussian filter. The modified Gaussian model is used to describe the vessel profile. The width of a vessel is obtained by data fitting. Significant differences between theirs and ours are follows: first, ours uses Canny edge detection that provides priori knowledge of the vessel boundaries and gradient orientations. Second, while both algorithms use the Gaussian model to describe the vessel profiles, ours uses Gaussian fit for each vessel sample and the edge positions are adjusted by finding a zeros cross position over the second order derivative of the Gaussian profile. Many vessel segmentation and measurement methods involve an enhancement process. In this method, the enhancement process is the first handled by convolution with derivative of Gaussian to remove image noise during the Canny edge detection. And second, the two-dimensional (2D) smoothing of vector field over the blood vessel wall positions, and third, the 1D smoothing of cross-sectional profiles of blood vessels.

EDGE EXTRACTION AND ORIENTATION ALIGNMENT

In our algorithm, when an edge position is found, a vessel cross-sectional profile is searched along the direction perpendicular to the orientation of the edge. By using the profile, a more accurate vessel wall position can be calculated, and the missing wall information from the other side can be recovered. The basic idea of searching for a vessel cross-sectional profile is illustrated in Fig. 1. A zoomed-in region of a retinal image is shown in part (a) of the figure. The vessel walls detected by Canny's edges are shown in part (b). A vessel cross-sectional profile is defined as the vessel crossing section of the image lies on the edge point perpendicular to the edge orientation.

For each edge along the vessel wall, an edge orientation can be determined and a cross-sectional profile can be searched. If a Gaussian model is used to fit the profile, a sub-pixel edge position can be found using zero cross of second order derivative of the Gaussian fit. The edge position of the other side of the vessel wall can also be estimated. In this idea, the orientation of the edge is critical. It requires that the orientation of each edge point be accurate, and the changes of the orientations of the edges along the vessel wall be smooth. Otherwise the neighborhood vessel sections may be crossing each other as shown in Fig. 2.

In that case, both the edge position and the center point position of the vessel profile can be misplaced. In order to solve this problem, in this algorithm, the edge orientation is defined as the direction of an edge moving along the vessel wall in a 2D space. A filter is used to smooth the orientations of the neighborhood edges. In Canny detection method, the direction of the gradient is $\theta=\tan^{-1}\left(\frac{\partial f}{\partial y}/\frac{\partial f}{\partial x}\right)$ where $\nabla f=\left[\frac{\partial f}{\partial y},\frac{\partial f}{\partial x}\right]$, (x,y) is the location of the pixel in the image and f is the pixel gray value. In our algorithm, the orientation of an edge is defined as a unit vector of

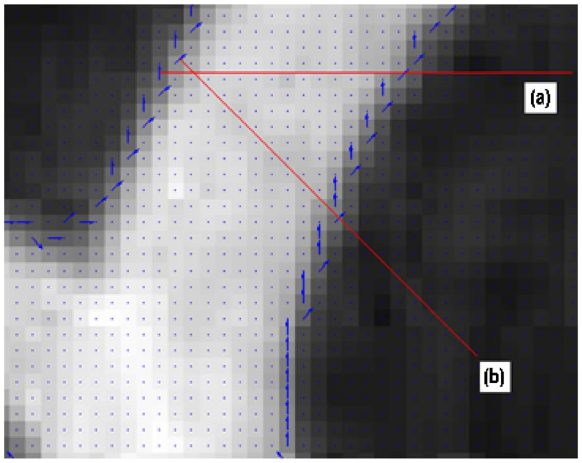

Figure 2. Edge orientations vector field over the vessel image based on vessel curve extracted from Canny edges. Note that the travel directions along the vessel wall are not smooth and the neighborhood vessel cross-sectional profiles (a) and (b) are crossing.

$$v = \left[\frac{dx}{du} \; \frac{dy}{du} \right]', \qquad (1)$$

where

$$C(u,r) = (x(u), y(u)) \qquad (2)$$

is the curve of the vessel wall where u is the index of the edges and r is the distance between two neighborhood edges. The curve of the vessel wall can be tracked from the result of Canny edges. A sample of the orientation of the edges from a vessel wall is shown in Fig. 2. The vectors of the edge orientation that form a vector field are plotted over the vessel image. One can see that the travel directions of the edge points along the vessel wall are not smooth. As a result, some neighborhood vessel cross-sectional profiles can be crossing.

The vectors of the edge orientation are pointing to a similar direction because the edges are detected based by pixel locally. The orientation of the vector can be aligned using either smoothing of the orientation or smoothing of the curves by following equations:

$$X(u,r) = \int_{-\infty}^{\infty} x(t) \frac{1}{r\sqrt{2\pi}} e^{-(u-t)^2/2r^2} dt \qquad (3)$$

and

$$Y(u,r) = \int_{-\infty}^{\infty} y(t) \frac{1}{r\sqrt{2\pi}} e^{-(u-t)^2/2r^2} dt, \qquad (4)$$

where the Gaussian path smoothing function of

$$g(u,r) = \frac{1}{r\sqrt{2\pi}} e^{-(u-t)^2/2r^2} \qquad (5)$$

is used. Equations (3) and (4) are the convolution of Gaussian smoothing function and the two functions $x(u)$ and $y(u)$.

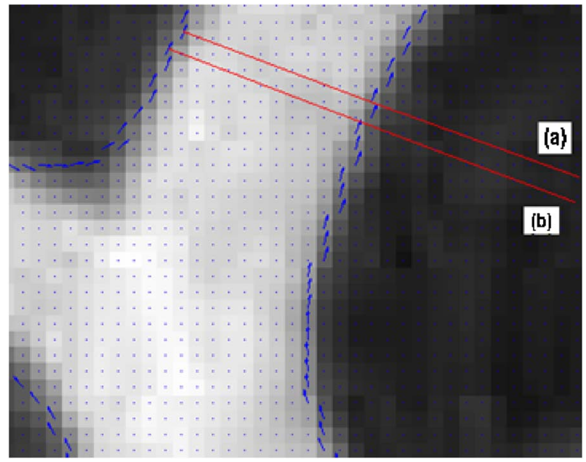

Figure 3. Edge orientations after alignment show small direction changes along the vessel wall. Note that the travel directions are smooth and the neighborhood vessel cross-sectional profiles (a) and (b) are not crossing.

Figure 3 shows the vector field of the edge orientation after the alignment using a seven-step 2D smooth process. The smoothed vector sequence is a function of its input vector sequence along the blood vessel curve as shown by Eq. (6)

$$m(u,v) = f(g(x,y)), \qquad (6)$$

where $m(u,v)$ is the smoothed vector sequence and $f(x,y)$ is the input vector sequence. The N-step smooth process can be expressed by Eqs. (7) and (8)

$$u_k = \frac{1}{N} \sum_{i=k-n}^{k+n} x_i, \qquad (7)$$

$$v_k = \frac{1}{N} \sum_{i=k-n}^{k+n} y_i, \qquad (8)$$

where k and i are the indexes of the vector sequences and n is the nearest integers towards minus infinity of $N/2$.

SUB-PIXEL EDGE LOCATION AND CENTER LINE POSITION ESTIMATION

Using the curve smoothing or sub-pixel Canny edge detection method one may be able to find more accurate vessel wall position. However, there is no knowledge of where the center line is and what the width of the vessel at the point is. To solve this problem, vessel cross-sectional profile can be a good solution.

Vessel Cross-Sectional Profile

With the Gaussian shaped property of the blood vessel cross-sectional profile, the sample of a vessel shape can be located by giving the location of an edge position and its corresponding vessel cross-sectional profile. To locate the sample of the vessel profile from the cross-sectional profile, the peak of the vessel needs to be found. In our algorithm, the peak of the vessel sample is defined as the local maximum closest to the edge point with a magnitude larger than

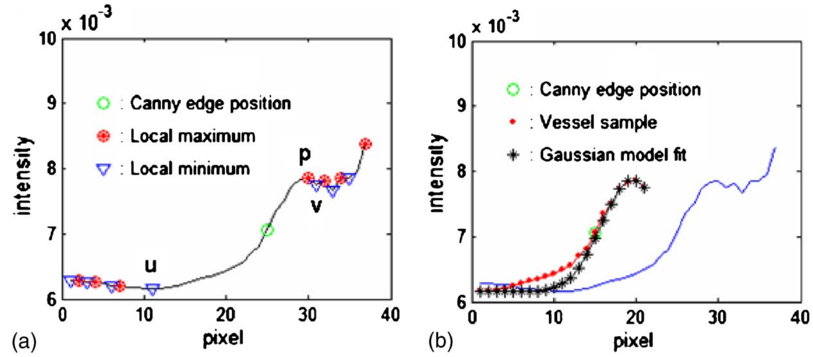

Figure 4. Vessel sample profile determination and Gaussian fit of the profile.

the magnitude of the edge point. The local maximum and local minimum are highly sensitive to noise. A 1D N-step smoothing process is used to prevent finding the maximum and the minimum at the wrong positions.

$$q_i = \frac{1}{N} \sum_{i=k-n}^{k+n} p_i, \tag{9}$$

where p is the cross-sectional profile, q is the smoothed cross-sectional profile, and i is the indexes and n is the nearest integers towards minus infinity of $N/2$. Then, the sample of the vessel profile is defined as the part of the cross-sectional profile between two neighborhood minimal points of the peak. Part (a) of Fig. 4 shows the locations of Canny edge point and local maximum and local minimum. Local maximum point p of the peak of the profile sample is first found and then, two neighbor minimums of u and v are located. Comparing the cross-section profile and the vessel sample profile, the curve contains local maximum p and between local minimums u and v is plotted and Gaussian fit for the sample profile is shown in part (b) of the figure.

Sub-Pixel Edge from Gaussian Fit of Vessel Cross-Sectional Profile

After using a Gaussian model to fit the sample profile, the sub-pixel edge position is estimated based on the zero cross of second order derivative of the Gaussian model. The location of the center line is selected as the peak of the Gaussian model.

Figure 5 shows the vessel cross-sectional profile obtained from a neighborhood of a vessel image based on Canny edge position.

One can see that the vessel sample profile is a sub set of vessel cross-sectional profile that contains two neighborhood local minimums of the edge positions. The Gaussian model is a smooth function slightly wider than the vessel sample in this case. A sub-pixel edge position is calculated using the zero cross of second order of derivative of the Gaussian model and is plotted out as a dot on the Gaussian fit curve. By comparing with the origin Canny edge location plotted out as a star on the vessel sample profile, the sub-pixel edge position shifts to the left hand side about 1 pixel from the Canny edge position. The peak of the Gaussian model is then used as the center line of the vessel and the width of the vessel at this point is calculated based on the center point and the new edge point.

Both positions of the sub-pixel edge and Canny edge over their local vessel image can be seen in Fig. 6. In the figure, the square mark shows the location of the Canny edge and the triangle mark shows the sub-pixel edge.

A set of the sub-pixel edge positions along a vessel is estimated using the above method and plotted out as dark

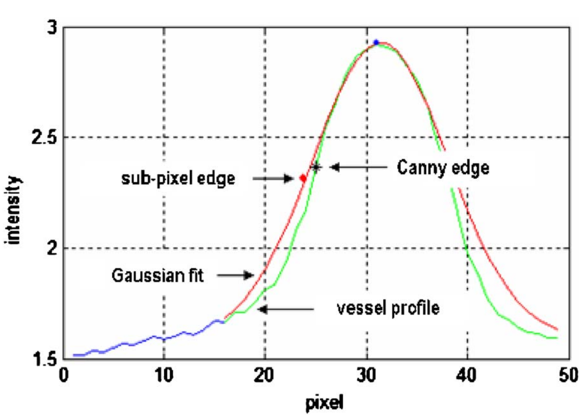

Figure 5. Sub-pixel edge position comparing with Canny edge position with respect to their corresponding vessel cross-sectional profile.

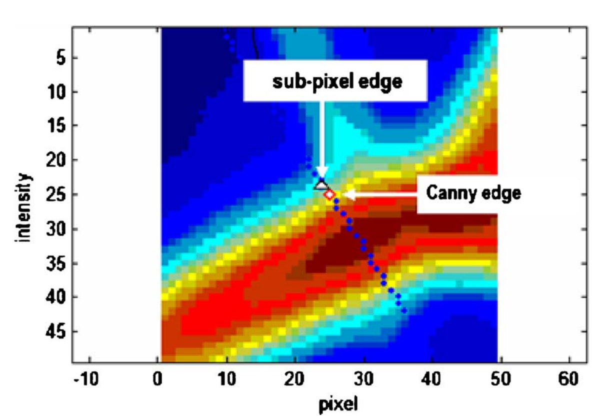

Figure 6. Gaussian fit moves the peak position of a vessel cross-sectional profile.

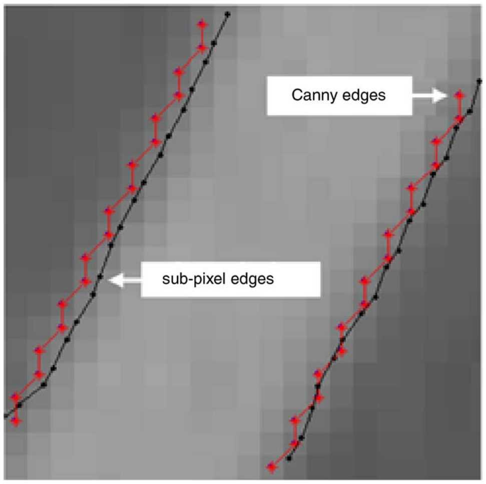

Figure 7. Different blood vessel boundaries detected using Canny edge detector and our algorithm.

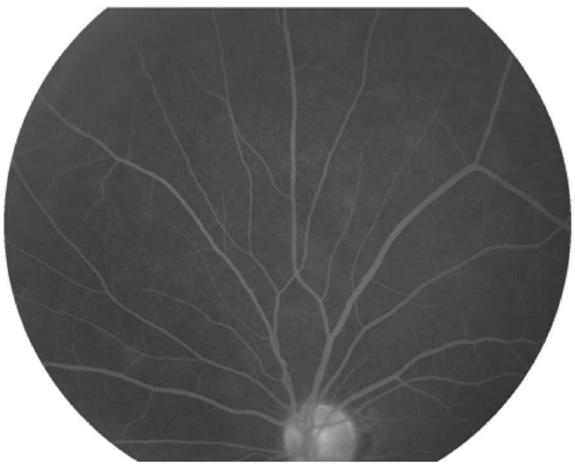

Figure 8. Scanned negative of red-free fundus image.

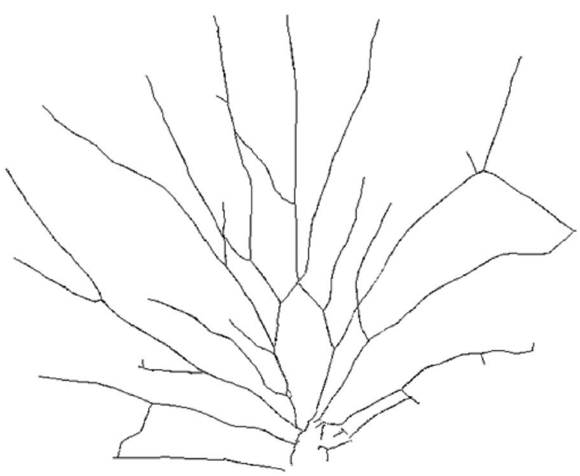

Figure 9. Extracted center line positions of the input blood vessel image.

dots in Fig. 7. Comparing with edge positions from Canny plotted out in stars, the sub-pixel edges appear forming smoother vessel walls.

The algorithm can be described as follows:

Table I. Experimental output sample data in pixel.

κ_x [a]	κ_y [a]	ψ_x [b]	ψ_y [b]	ϕ_x [c]	ϕ_y [c]	λ [d]
669	26	669.1626	27.0188	666	27.0900	6.3252
508	27	509.0222	27.9960	506	28.5370	6.0443
669	27	669.1078	28.0254	666	28.1140	6.2156
669	28	669.1409	29.0292	666	29.1357	6.2819
669	29	669.1584	30.0332	666	30.1580	6.3167
508	30	509.6108	30.9230	507	31.2521	6.2216
669	30	669.1737	31.0381	666	31.1842	6.3473
669	31	669.1921	32.0440	666	32.2177	6.3841
669	32	669.2188	33.0508	666	33.2601	6.4375
509	33	511.2986	33.7165	508	34.4367	6.5972
669	33	669.3123	34.0535	666	34.3113	6.6246
669	34	669.3459	35.0604	666	35.3696	6.6918
510	35	512.1432	35.5679	509	36.7559	6.2865
669	35	669.3555	36.0696	666	36.4323	6.7110
669	36	669.4276	37.0710	666	37.4961	6.8552
868	36	869.0395	37.0200	866	35.4838	6.0790
669	37	669.4639	38.0748	666	38.5582	6.9279
867	37	868.3686	38.1705	865	36.6121	6.7373
866	39	867.4067	40.1525	864	38.8748	6.8134

[a] (κ_x, k_y): Blood vessel wall locations from Canny edge detection;
[b] (ψ_x, ψ_y): blood vessel locations from our algorithm;
[c] (ϕ_x, ϕ_y): center line locations using our algorithm;
[d] λ: width of the blood vessel using our algorithm.

(1) Use Canny edge detection method to extract the edges along the vessel from the input image;
(2) Track all curves $C(u,r)$ of Eq. (2) from the Canny edge image;
(3) Smooth the curves use either the multiple step smoothing or 2D curve smoothing equation of Eqs. (3) and (4).
(4) Obtain the orientation vectors of the edge point using Eq. (1) along the smoothed curves;
(5) Select a window size larger than twice of maximal width of the vessels. For each edge pixel, a sub image within the window around the edge is used to extract the vessel cross-sectional profile.
(6) Determine the vessel sample profile using the peak point and its neighborhood minimums.
(7) Obtain Gaussian fit with the vessel sample profile.
(8) Use zero cross of the second order derivative of the Gaussian fit to obtain the sub-pixel position of the edge.

EXPERIMENT

The algorithm presented in this paper was implemented using MATLAB and tested with real images. A set of 53 test images of 1032×1302 pixels was randomly selected. A sample of test image is shown in Fig. 8. A Gaussian filter with kernel of 1 is used to smooth the image. Then, the Canny edge detector with a threshold value of 0.1 is used to detect the edge points. A total number of 16,775 edge points were detected from the sample image.

A function to track the edge positions into a set of curves is used to record the edge points along different curves. For each curve, a seven-step smoothing process is then used to smooth the curves. An orientation vector is calculated using Eq. (1) based on the smoothed edge positions along the curve and is assigned to each edge point. For each edge point, its corresponding orientation vector is then used to select a vessel cross-sectional profile. In this experiment, a window size of 50 pixels is used to select the vessel cross-sectional profile. For each profile, a sample segment of the profile is found using local minimums and a Gaussian fit is then achieved. The new edge with sub-pixel precision is calculated using zero cross of second order derivative of the Gaussian fit.

The results of the algorithm include the Canny edge locations, the sub-pixel edge positions estimated from the Gaussian fit and the peak positions of the Gaussian fit is used to represent the sub-pixel edge and the width of the vessel at this point is calculated based on the distance between the sub-pixel edge position and the peak of the Gaussian fit model. The plot out of the center line positions is shown in Fig. 9 and a set of output data samples is shown in Table I. In the table, (κ_x, κ_y) show blood vessel wall locations from Canny edge detection. We can see the locations of the blood vessel walls are pixel based with integer x and y index. (ψ_x, ψ_y) show the blood vessel wall locations from our algorithm with sub-pixel accuracy. (ϕ_x, ϕ_y) show the center line locations of the blood vessels using our algorithm. The results of center line estimation of all (ϕ_x, ϕ_y) are plotted and shown in Fig. 8.

CONCLUSIONS

We have presented an efficient approach to track retinal vessel center lines and to measure the width of the vessel at each center point using modified Canny edge detection method. Our algorithm improves previous approaches by refining edge orientation and using Gaussian model to fit the vessel cross-sectional profile. The sub-pixel edge positions are then obtained from the Gaussian model and accurate vessel center line positions are then calculated based on the center points. Both Gaussian fit and the local maximum of second order derivative of Gaussian fit are optimal. Therefore the accuracy of the vessel tracking and measurement is guaranteed.

The experimental show well results in measurements on vessels width larger than 4 pixels because it is difficult to detect the edges of both large and small vessels using Canny edge detector with same Gaussian kernel and Canny hysteresis thresholdings. A filter designed to extract edges of smaller vessels will be presented in a separated paper.

ACKNOWLEDGMENT

This research was supported by MIC (the Ministry of Information and Communication, Korea) under the Foreign Professor Invitation Program of the IITA (Institute for Information Technology Advancement).

REFERENCES

[1] C. Kirbas and F. Quek, “Vessel extraction techniques and algorithm: a survey”, *Proc. 3rd IEEE Symposium on BioInfomratics and Bioengineering (BIBE’ 03)* (IEEE, Piscataway, NJ, 2003).

[2] T. M. Koller, G. Gerig, G. Szekely, and D. Dettwiler, “Multipscale detection of curvilinear structures in 2-D and 3-D image data,” *Proc. Fifth Int’l Conf. of Computer Vision* (1995) 864–869.

[3] J. B. Subirana-Vilanva and K. K. Sung, “Multi-scale vector-ridge detection for perceptual organization without edges”, *AI Memo No.* 1318 (MIT Artif. Intel. Lab. Cambridge, MA, 1992).

[4] L. Wang and T. Pavlidis, “Direct gray-scale extraction of features for character recognition”, IEEE Trans. Pattern Anal. Mach. Intell. **15**, 1053–10367 (1993).

[5] L. A. Iverson and S. W. Zucker, “Logical/linear operators for image curves”, IEEE Trans. Pattern Anal. Mach. Intell. **17**, 982–996 (1995).

[6] J. Maintz, P. Elsen, and M. A. Viergever, “Evaluation of ridge seeking operators for multimodality medical image matching”, IEEE Trans. Pattern Anal. Mach. Intell. **18**, 353–365 (1996).

[7] J. Canny, “A computational approach to edge detection”, IEEE Trans. Pattern Anal. Mach. Intell. **8**, 679–697 (1986).

[8] W. Pratt, *Digital Image Processing* (Wiley, New York, 1978).

[9] Y. Qian, S. Eiho, N. Sugimoto, and M. Fujita, “Automatic extraction of coronary artery tree on coronary angiograms by morphological operators”, Comput. Cardiol. **25**, 765 (1998).

[10] Y. Sun, “Automated identification of vessel contours in coronary arteriogram by an adaptive tracking algorithm”, IEEE Trans. Med. Imaging **8**, 78–88 (1989).

[11] H. Can, H. Shen, J. Turner, H. Tanenbaum, and B. Roysam, “Rapid automated tracing and feature extraction from retinal fundus images using direct exploratory algorithms”, IEEE Trans. Inf. Technol. Biomed. **3**, 125–138 (1999).

[12] P. M. Zwet, M. Nettesheim, J. Gerbrands, and J. Reiber, “Derivation of optimal filters for the detection of coronary arteries”, IEEE Trans. Med. Imaging **17**, 108–120 (1998).

[13] L. Gang, O. Chutatape, and S. M. Krishnan, “Detection and measurement of retinal vessels in fundus images using amplitude modified second-order Gaussian filter”, IEEE Trans. Biomed. Eng. **49**(2), 168–172 (2002).

[14] M. Sofka and C. Stewart, “Retinal vessel centerline extraction using multiscale matched filters, confidence and edge measures”, IEEE Trans. Med. Imaging **25**, 1531–1546 (2006).

[15] R. Ravhon, D. Adam, and L. Zelmanovitch, “Validation of ultrasonic image boundary recognition in abdominalaortic aneurysm”, IEEE Trans. Med. Imaging **20**, 751–763 (2001).

[16] M. Shoura and O. Alim, “A new method for dynamic road mapping of coronary angiography cardiac catheterization cine loops”, *Proc. 25th Annual International Conf. IEEE Engineering in Medicine and Biology Society* (IEEE, Piscataway, NJ).

[17] D. R. Adam and R. Ravhon, “Echo ultrasound measurement of lumen size in aortic aneurysm”, Comput. Cardiol. **25**, 77–80 (1998).

[18] M. Nixon and T. Hames, “New technique for 3D artery modeling by noninvasive ultrasound”, IEEE Proc. Communications, Speech and Vision **140**, 86–94 (1993).

[19] P. Zwet, M. Nettesheim, J. Gerbrands, and J. Reiber, “Derivation of optimal filters for the detection of coronary arteries”, IEEE Trans. Med. Imaging **17**, 108–120 (1998).

[20] M. Hafez and S. Azeem, “Using adaptive edge technique for detecting microaneurysms in fluorescein angiograms of the ocular fundus”, *11th Mediterranean Electrotechnical Conference, MELECON 2002*, 479–483 (2002).

[21] A. Hamou and M. El-Sakka, “A novel segmentation technique for carotid ultrasound images”, *Proc. IEEE International Conference on Acoustics, Speech, and Signal Processing* (IEEE, Piscataway, NJ, 2004), Vol. **3**, iii; 521–524.

[22] J. Gao and W. Quan, “Automatic 3D vascular tree construction of perforator flaps for plastic surgery planning”, *Proc. 26th Annual International Conf. IEEE Engineering in Medicine and Biology Society* (IEEE, Piscataway, NJ, 2004), Vol. **2**, 3424–3427.

[23] L. Zhou, M. S. Rzeszotarski, L. J. Singerman, and J. M. Chokreff, “The detection and quantification of retinopathy using digitalangiograms”, IEEE Trans. Med. Imaging **13**, 619–626 (1994).

[24] H. Li, W. Hsu, M. L. Lee, and T. Y. Wong, “Automatic grading of retinal vessel caliber”, IEEE Trans. Biomed. Eng. **52**(7), 1352–1355 (2005).